DEVELOPMENT OF SCHEMATIC DESIGN MODEL OF GANTRY CRANE FOR DYNAMIC ANALYSIS AND REGULATION OF TRAVEL MOTION

Prof.asc. Doçi Ilir, Prof.asc. Lajqi Naser*
Faculty of Mechanical Engineering –University of Prishtina, Kosovo (ilir.doci@uni-pr.edu)
*Corresponding author (naser.lajqi@uni-pr.edu)

Abstract: *This paper deals with Dynamic analysis of Gantry Crane using Method of Schematic Design which implements schemes with block diagrams to analyze machines and their parts during work process. This procedure is new to analysis of Gantry crane dynamics and consists of crane model development of interconnected elements that represents crane parts, 3-D visualization and motion of crane. Dynamic analysis will be carried through simulations and solution of Euler differential equations of second order gained from schematic design. Simulations will be planned and applied for regulation of travel motion with hanging load. Diagrams with results of main dynamic and kinematic parameters will be presented for main parts of crane as the solution results of the analyzed system. Results gained will be used to get conclusions about dynamic behavior, optimal motion regulation and safety during work. Analysis will be done using modeling and simulations with computer application MapleSim.*

Keywords: GANTRY CRANE, SCHEMATIC DESIGN, DYNAMIC ANALYSIS, TRAVEL MOTION, REGULATION, MODELING, SIMULATIONS

1. Introduction

Gantry crane is modeled based on manufacturer *Kren vinç KR - 12H* (Fig.1)[1]. Crane is mounted in rails in basement. Max carrying load $Q = 10000$ *kg*. Total Length of girders $L = 16+6=22$ *m (*Fig.2). Height of girders H = 7.8 m. Weight of each of 2 girders 3000 kg. Weight of one leg 2400 kg. Distance between legs: 16 m. Height of legs 8 m (Fig.2). Velocity of crane $v_{cr} = 0.25$ *m/s*. Diameter of crane wheels D_v = 200 mm. Crane is moving on 4 wheels per each leg. Before simulations, weight Q (workload) is in the position of relative rest at the height H = 3 m from basement. Simulations will be done for crane traveling - translational motion for time t = 15 s, which converts to travel length l = 3.75 m.

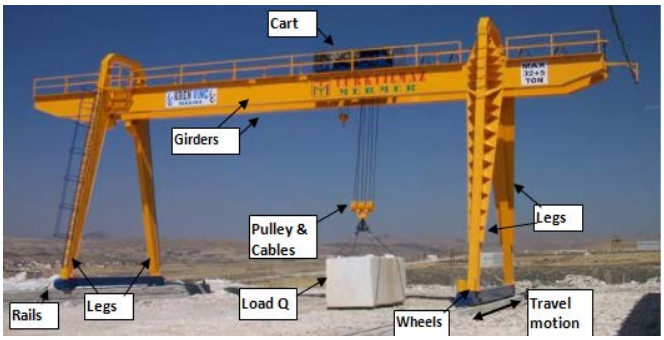

Fig.1. Gantry crane with parts [1]

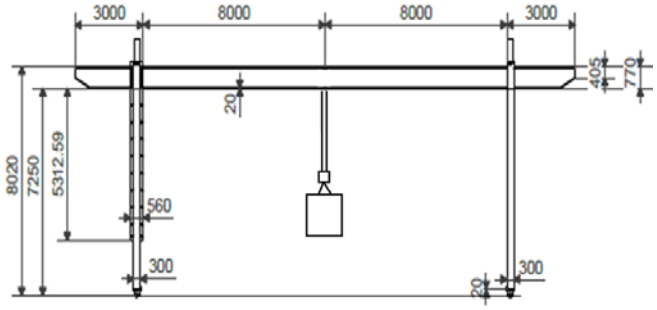

Fig.2. Gantry crane main dimensions [1]

2. Schematic design of Gantry crane

In Fig.3 is presented schematic design and block diagram of Gantry crane created with software that enables topological representation and interconnects related components [5]. Schematic diagram is created in order to create model, generate differential equations, apply simulations and make analysis [4],[5].

Crane parts are designed with these schematic elements, starting from left (index *l)* to right (index *r)* (Fig.3):

- ***Rigid body frames (bars):*** Basement Link Bars- *Lb1, Lb2, rb1, rb2*; Crane Legs – *ll1, ll2, lu1, lu2, lmu1, lr1, lr2, ru1, ru2, rmu1*; Front Girder – *Grl1, Grr1*; Rear Girder – *Grl2, Grr2*; Cart bars – *bm1, Bm2, bm3, bm4*; Traverse- *Tr1, Tr2*; Hanging cables – *ro1*.
- ***Concentrated masses*** – Basement Masses – *mwl1, mwl2, mlb, mwr1, mwr2, mrb*; Crane Legs – *mll1, mll2, mlr1, mlr2*; Front Girder – *ml1, mr1, m1, m3*; Rear Girder – *ml2, mr2, m2, m4*; Cart- *c1, c2*; Pulley – *P1, P2*; Traverse – *mtr*; Load-*Q*;

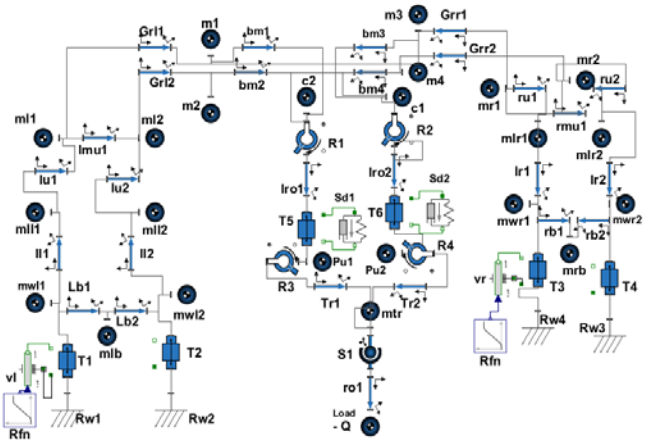

Fig.3. Block Diagram of gantry crane with travel motion

- ***Fixed Frames*** – Basement of crane – *Rw1, Rw2, Rw3, Rw4*;
- ***Revolute joints***- *R1, R2, R3, R4*; *Spherical joint- Hook - S1*;
- ***Pistons***: Lifting Boom piston- P1; Telescopic Boom piston - P2;
- ***Lifting cables*** - are created with link beams *lro1, lro2,* Spring and dumping elements - *Sd1 & Sd2*, and translational joints *T5, T6*. Together with Load *Q*, Hanging cables – ro1, Traverse – *Tr1, Tr2*, and Hook – *S1* are modelled in the form of double pendulum.
- **Velocity generators** – *vl, vr;* **Ramp functions**- *Rfn*.

In Fig.4. is presented discrete-continuous model of crane used for model view and simulation. This model is 3-D visualization created by software recurring from Block diagram on Fig.2. On this model simulations will be performed in time frame of $0< t < 10$ s. During this simulation time, crane will lift up Boom and Load Q.

3. Differential equations of Gantry-crane motion

To formulate dynamics of this system, standard Euler-Lagrange methods are applied, by considering the crane as a multi-body system composed by links and joints. For a controlled system with several degrees of freedom (DOF), the Euler-Lagrange equations are given as [2], [4], [6]:

$$\frac{d}{dt}\left(\frac{\partial E_k}{\partial \dot{q}_i}\right)+\frac{\partial E_p}{\partial q_i}=Q_i \qquad \text{(i=1 ,2...n)} \qquad (3.1)$$

Where: $\mathbf{q_i}$ - are generalized coordinates for the system with n degrees of freedom, $\mathbf{E_k}$ is Kinetic Energy, $\mathbf{E_p}$ is Potential energy, $\mathbf{Q_i}$ is the n-vector of external non-conservative forces acting at joints.

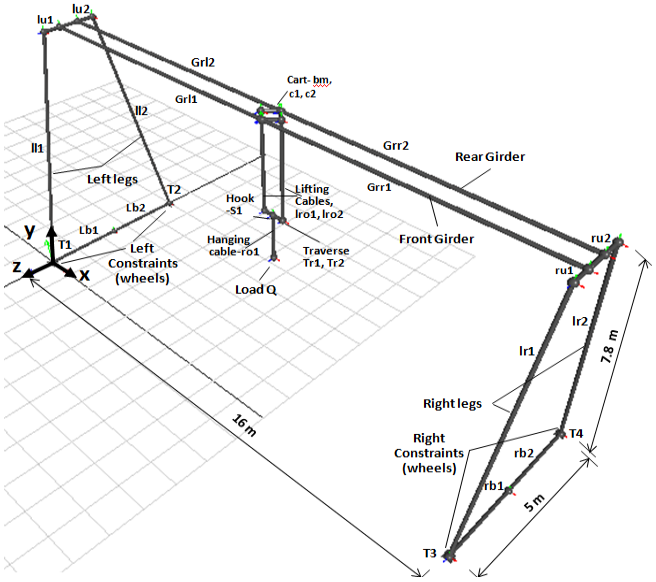

Fig.4. Discrete-continuous model of gantry-crane

Kinetic energy for mechanical systems is in the form*:*

$$E_k(q,\dot{q}) = \frac{1}{2}\dot{q}^T \cdot M(q) \cdot \dot{q} \qquad (3.2)$$

$E_p(q)$ – is potential energy that is a function of systems position.

M(q) - is a symmetric and positive matrix of inertias. [6]

Modern software's calculates physical modeled systems through mathematical methods, numeric methods and Finite Elements Method. These calculations are based on Euler-Lagrange Equation (3.1), and forces applied for control of force/moments acting on crane. The crane dynamic equations can be written in the following second order differential equation:

$$M(q)\cdot\ddot{q}+C(q,\dot{q})\dot{q}+\frac{\partial E_p}{\partial q}=Q(q,\dot{q})-B^T u \qquad (2.3)$$

where **M** is the *nx n* generalized mass matrix, $C(q,\dot{q})$ is *nxn* matrix of Corriolis Forces, $\mathbf{\delta E_p/\delta q}$ is the vector of gravity, **Q** is *n*-vector of generalized applied forces, and $\mathbf{B^T}$ is the *nxm* matrix of influence of control inputs **u** on the generalized force vector $\mathbf{f_u = -B^T u}$ created by speed generator [6].

After completion and testing of model, Software Maplesim has powerful module for symbolic generation of differential equations [3]. There are 19 DOF for crane model (Fig.3), which gives 19 differential equations. Variables in differential equations given in time dependency are:

ζ(t) – Position of load Q around *x* axis; ***η (t)*** – Position of load Q around *y* axis; ***ξ(t)*** – Position of load Q around *z* axis; ***T1_F(t)*** – force in translational joint T1; ***T3_F(t)*** – force in translational joint T3; ***T5_F(t)*** – force in translational joint T5; ***T5_s(t)*** – motion in translational joint T5; ***T6_F(t)*** – force in translational joint T6; ***T6_F1(t)*** – force 1 in translational joint T6; ***vl_a(t)*** – acceleration caused by left speed generator *vl;* ***vl_v(t)*** – velocity caused by left speed gjenerator *vl;* ***vl_s(t)*** – travel caused by left speed generator *vl;* ***vr_a(t)*** – acceleration caused by left speed generator *rl;* ***vr_v(t)*** – velocity caused by left speed generator *vr;* ***vr_s(t)*** – travel caused by left speed generator *vr;* ***R1_θ(t)*** – Rotation of Revolute joint R1 around its axis (z), (Euler Angles); ***R2_θ(t)*** – Rotation of Revolute joint R2 around its axis (z); ***R3_θ(t)*** – Rotation of Revolute joint R3 around its axis (z); ***SD2 _s_rel(t)*** – Relative length of lifting cables SD2.

3.1. Differential equations

19 Differential equations that represent lifting motion of crane are very long, and we will be presented in short form:

$$-\frac{1}{10000}\frac{d}{dt}\left(\frac{d}{dt}\text{R2\_}\theta(t)\right)+\frac{1}{10000}\frac{d}{dt}\left(\frac{d}{dt}\text{R3\_}\theta(t)\right)=0 \qquad ...(3.1.1)$$

$$\text{-T5\_F(t)-300000}\cdot\text{T5\_s(t)-4000}\cdot\left(\frac{d}{dt}\text{T5\_s(t)}\right)=0 \qquad ...(3.1.2)$$

$$\text{-T3\_F(t)-}\sin(\text{R2\_}\theta(t))\cdot\text{T6\_F(t)+}\cos(\text{R2\_}\theta(t))\cdot\text{T6\_F1(t)}$$
$$+5800\cdot\frac{d}{dt}\left(\frac{d}{dt}\text{vr\_s(t)}\right)=0 \qquad ...(3.1.3)$$

$$\cos(\text{R1\_}\theta(t))\cdot\text{T5\_s(t)})\cdot\sin(\text{R2\_}\theta(t))\text{- T5\_s(t)})\cdot\cos(\text{R2\_}\theta(t))\cdot$$
$$\sin(\text{R1\_}\theta(t))+3\cdot\cos(\text{R1\_}\theta(t))\cdot\sin(\text{R2\_}\theta(t))\text{- 3}\cdot\cos(\text{R2\_}\theta(t))\cdot$$
$$\sin(\text{R1\_}\theta(t))+\cos(\text{R2\_}\theta(t))\cdot\text{vr\_s(t)}=0 \qquad ...(3.1.4)$$

$$\frac{1}{10000}\frac{d}{dt}\left(\frac{d}{dt}\text{R2\_}\theta(t)\right)+\text{T6\_F(t)})\cdot\cos(\text{R1\_}\theta(t))\cdot\text{T5\_s(t)})\cdot$$
$$\sin(\text{R2\_}\theta(t))\text{- T6\_F1(t)})\cdot\cos(\text{R1\_}\theta(t))\ \text{T5\_s(t)})\cdot\cos(\text{R2\_}\theta(t))+3\cdot$$
$$\text{T6\_F1(t)})\cdot\cos(\text{R1\_}\theta(t))\cdot\sin(\text{R2\_}\theta(t))\text{-...- T6\_F1(t))}\cdot\sin(\text{R2\_}\theta(t))\cdot$$
$$\text{vr\_s(t)}=0 \qquad ...(3.1.5)$$

$$45000\cdot\sin(\xi(t)\cdot\cos(\xi(t))\cdot\left(\frac{d}{dt}\eta(t)\right)\cdot\left(\frac{d}{dt}\xi(t)\right)+30000\cdot$$
$$\cos(\zeta(t))\cdot\sin(\xi(t))\cdot\cos(\eta(t))\cdot\left(\frac{d}{dt}\left(\frac{d}{dt}\text{R1\_}\theta(t)\right)\right)\cdot\cos(\text{R1\_}\theta(t))\text{-}$$
$$...+22500\cdot\sin(\xi(t))\cdot\cos(\eta(t))\cdot\cos(\xi(t))\cdot\left(\frac{d}{dt}\left(\frac{d}{dt}\zeta(t)\right)\right)=0 \qquad ...(3.1.6)$$

$$\text{- T1\_F(t)}+30000\cdot\left(\frac{d}{dt}\xi(t)\right)^2\cdot\sin(\zeta(t))\cdot\cos(\xi(t))+30000\cdot\sin(\eta(t))\cdot$$
$$\left(\frac{d}{dt}\eta(t)\right)^2\cdot\sin(\xi(t)\cdot\cos(\zeta(t))+15000\cdot\cos(\zeta(t))\cdot\left(\frac{d}{dt}\xi(t)\right)^2\cdot\sin(\xi(t)\cdot$$
$$\sin(\eta(t))+...+15000\cdot\sin(\xi(t))\cdot\cos(\eta(t))\cdot\cos(\zeta(t)\cdot\left(\frac{d}{dt}\left(\frac{d}{dt}\eta(t)\right)\right)$$
$$+15000\cdot\sin(\eta(t))\cdot\cos(\zeta(t)\cdot\sin(\xi(t))\left(\frac{d}{dt}\zeta(t)\right)^2=0 \qquad ...(3.1.7)$$

….

$$\left(\frac{d}{dt}(\text{vl\_v(t)})=\text{vl\_a(t)}\right. \qquad ...(3.1.12)$$

$$\left(\frac{d}{dt}(\text{vr\_v(t)})=\text{vr\_a(t)}\right. \qquad ...(3.1.13)$$

$$\frac{d}{dt}\text{SD2\_s\_rel(t)}=-\frac{1}{4000}\cdot\text{T6\_(F(t)-75}\cdot\text{SD2\_s\_rel(t)} \qquad ...(3.1.14)$$

$$\text{vl\_a(t)}=100\cdot\left(\frac{1}{8}\tanh(\text{t-3})+\frac{1}{8}\text{ - vl\_v(t)}\right)\cdot\pi \qquad ...(3.1.15)$$

$$\text{vl\_v(t)}=\left(\frac{d}{dt}(\text{vl\_s(t)})\right. \qquad ...(3.1.16)$$

$$\text{vr\_a(t)}=100\cdot\left(\frac{1}{8}\cdot\tanh(\text{t-3})+\frac{1}{8}\text{ - vr\_v(t)}\right)\cdot\pi \qquad ...(3.1.17)$$

$$\text{vr\_v(t)}=\left(\frac{d}{dt}(\text{vr\_s(t)})\right. \qquad ...(3.1.18)$$

$$\text{SD2\_s\_rel(t)}=\cos(\text{R1\_}\theta(t))\cdot\text{T5\_s(t)})\cdot\cos(\text{R2\_}\theta(t))+\text{T5\_s(t)})\cdot$$
$$\sin(\text{R2\_}\theta(t))\cdot\sin(\text{R1\_}\theta(t))+3\cdot\cos(\text{R1\_}\theta(t))\cdot\cos(\text{R2\_}\theta(t))\text{- 3+3}\cdot$$
$$\sin(\text{R1\_}\theta(t))\cdot\sin(\text{R2\_}\theta(t))\text{- }\sin(\text{R2\_}\theta(t))\cdot\text{vl\_s(t)} \qquad ...(3.1.19)$$

4. Experimental measurements

Measurements in crane are done in place of work, where crane is mounted, in one local company (Fig.1). They will be used for validation of results. Main measured parameter was force in hanging ropes – ***Fh*** *(Fy)*. It was measured with dynamometer type *Dini Argeo* attached to the Hook [8], during motion of crane (Fig.5). There were 5 measurements achieved, and results are shown in Table.1:

Time (s)	Force in hanging cables - Fh (N)
1	112000
5	103000
8	96000
11	97500
15	99000

Table 1. Results of Fh (Fy) with dynamometer in hanging cables

Fig.5. Measurements with Dynamometer during motion of crane

5. *Graphical results for main parts of crane*

Based on model created, differential equations gained, and simulations, results are achieved for main dynamic parameters [4], [7]: *Velocity (v) (m/s), Acceleration (a) (m/s^2), Angular velocity (w) (1/s), Angular acceleration (aa) (1/s^2), Force (F) (N), Force Moment-Torque (T) (Nm)*. Results are achieved after simulations applied on designed system, Fig.3 & Fig.4. Simulations are planned to reflect real travel of crane in order to achieve reliable results and comparable with measurements. Simulation has three phases (Fig.6) [4],[7]:

First phase – Initial travel. Velocity of crane v_t = 0…0.03 m/s. Time of travel 0 s <t < 2 s. *Second phase* – Velocity increase of travel, v_t = 0.03…0.25 m/s. Time of travel 2 s <t < 6 s. *Third phase* – constant velocity of travel v_t = 0.25 m/s . Starts after second phase, lasts between time 6 s <t< 15 s, which is end of simulation.

Simulation of crane travel is achieved with adjustment of travel velocity with ramp function **Rfn (**Fig.6, Fig.3). In practice, this velocity is not entirely constant, but close to the curve in Fig.6. Regulation of travel motion is achieved through numerous tests to implement planned simulation and achieve velocity $v_t \approx 0.25$ m/s, in order to get best results with less oscillations [4], [7]. This is the main process of regulation and control in this paper. Other parameters important for regulation are for hoisting mechanism - elements SD1, T5, and SD2, T6, in order to minimize effect of vibrations which appears in lifting cables and girders during motion [7]. Spring constant for SD1 and SD2 is determined with values **k = 3·10^5 N/m** and Damping constant is **d = 4000 Nm/s** [4].

Next will be presented graphical results for main parts of crane, where horizontal axis is time (t = 0…15 s) and vertical axes are corresponding values of dynamic and kinematic parameters. Only most significant graphs will be shown.

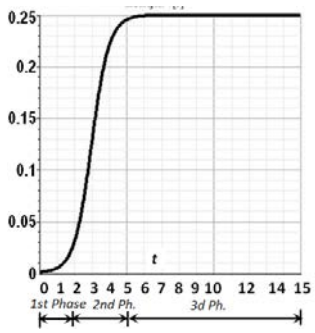

*Fig.6. Ramp function **Rfn** of speed v(z)*

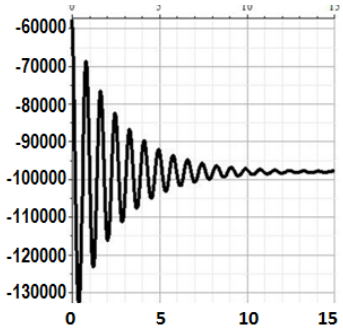

Fig.7. Force Fh (Fy) in hanging cables (ro1)

5.1. Results for hanging cables ro1 and Load Q

Hanging cables (or ropes) - **ro1** and load **Q** are connected and are components being carried by crane. Load Q makes swinging motion and oscillations during travel motion. This behavior influences directly and indirectly other parts of crane. Results of main parameters are shown in Fig.7, 8, 9. It is important to identify dynamic behavior of carried load in order to understand dynamic occurrences that affect other parts of crane.

Fig.7 represents vertical force *Fy* in hanging cables **ro1**. Force *F(y)* is Componential Force towards *y* axis. It has medium values of *F(y)* ≈ |-98000| N, which validates results with measurements in *Tab.1*. In this case values of other Forces *F(x)* or *F(z)* are very small and will not be shown in graphs. In Fig.8 and Fig.9 are shown kinematic parameters for load *Q*. In Fig.8, velocity components *v(y)* and *v(z)* shows that load *Q* has irregular motion and irregular oscillations. *v(y)* is very intense at the start of motion, due to swinging of load toward y axes, but after time t≈11 s it has low oscillations. *v(z)* is velocity towards motion of crane – *z* axes, and has oscillations with medium periods.

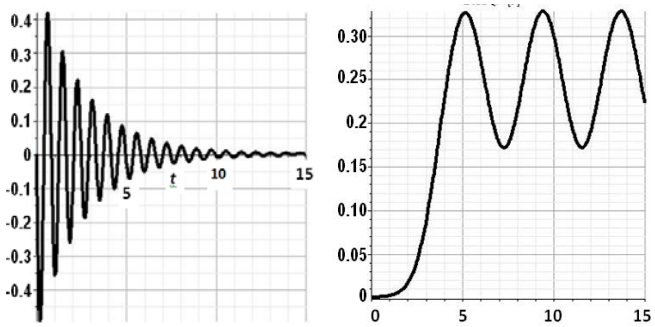

Fig.8. Load Q – Velocity v(y) and v(z)

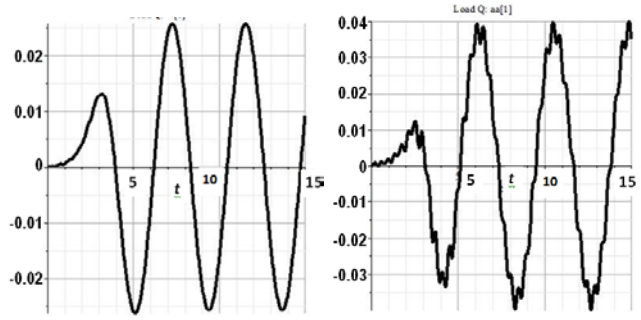

Fig.9. Load Q – angular velocity w(x) and angular accel. α(x)

Fig.9 represents angular velocity *w(x)* and angular acceleration *α(x)* of load Q. Graph shows dynamic form of these parameters, in a form of sinusoids, with medium periods, and oscillations with medium frequencies and amplitudes.

5.2. Results for lifting cables

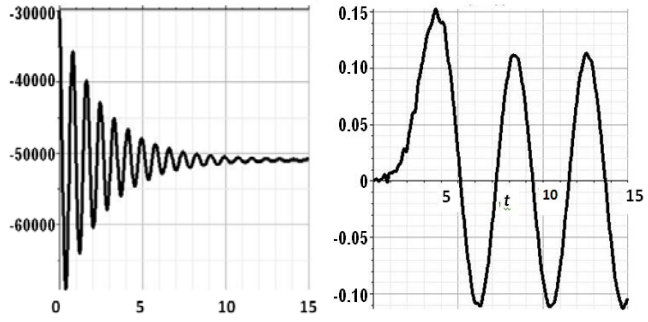

Fig.10. Lifting cables – Force F(y) and Acceleration a(z)

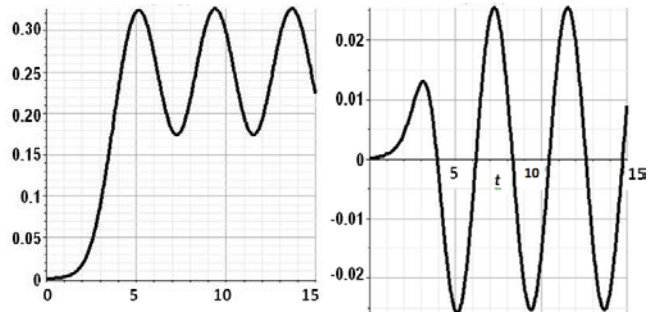

Fig.11. Lifting cable - Velocity v(z) and angular velocity w(z)

In schematic model (Fig.3) there are two lifting cables with objects *R1, R2, lro1, lro2, T5, T6, R3, R4*. They are the link between Cart (*c1* and *c2*) and traverse *Tr*. In Fig.10. are shown graphs of: vertical force in one cable - *F(y)*, Acceleration *a(z)*. Graph of Force *F(y)* has dynamic occurrence with amplitudes up to $\lambda_{Fy} \approx 1.4 \cdot 10^4$ N, and frequencies $\nu \approx 1.2$ Hz, which drops significantly after t=10 s. This is the intention of regulation of force in cables. Velocity v(z) and Angular velocity graphs *w(z)* (Fig.11) are similar as for load Q.

5.3. Results for Crane's Base and wheels

Wheels are mounted in base of crane, and are used for motion of crane (Fig.1). In diagram (Fig.3) Base and wheels are represented with elements *T1, T2, T3, T4* and masses *mwl1, mwl2, mlb, mwr1, mwr2, mrb*. In Fig. 12 is shown graph of vertical Force *F(y)* in front left wheels–*T1*. Values for other wheels are similar. Based on Fig.12, maximal value of force is F_{ymax} =63000 N, and medium value is F_y =53000 N. We can conclude that Base and wheels undergo heavy and irregular oscillations, with high amplitudes at the start, up to $\lambda_{Fy} \approx 1 \cdot 10^4$ N, and drops after t=10 seconds to almost $\lambda_{Fy} \approx 0$. This is the intention of regulation of travel motion.

In Fig. 13 is graph of Force *F(z)* in Front Left wheels T1 towards *z* axes. There should be no *F(z)* in wheels while there is free motion towards *z*, but due to swinging of load Q and hoist, the *F(z)* will appear with small intensity, but dynamic in form of sinusoid, with amplitude λ_{Fy} =1500 N. In Fig. 14 is graph of Torque around *x* axes-*T(x)*. It has max value: $T_{xmax} \approx 5.8 \cdot 10^4$ Nm at the start of process. Oscillations are heavy, with amplitudes that are high up to $\lambda_{Tx} \approx 8000$ N, with high frequencies, and drops after until t≈7 s with less but irregular frequencies. In Fig. 15 is graph of acceleration *a(z)* on left wheels. Max value is $a(z)_{max} \approx 0.13$ m/s^2 reached at time t≈ 3 s, and then drops at zero after t=6 s. Acceleration is result of the velocity regulation.

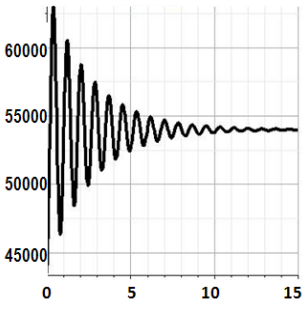

Fig.12. Force component F(y)

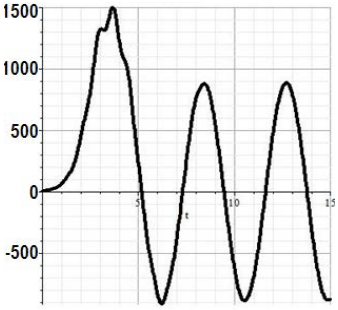

Fig.13. Left wheels–Force F(y)

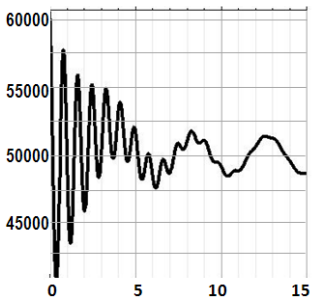

Fig.14. Left wheels-Torque T(x)

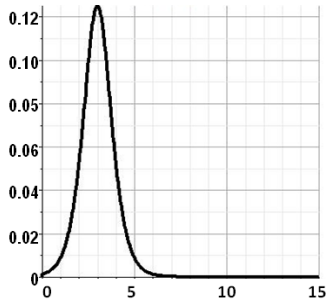

Fig.15. Acceleration a(z)

5.4. Results for Crane's Girders

Girders are considered most important part of Crane (Fig.1). On girders is mounted Cart that travels in rails, which has also mounted hoisting mechanism and load Q. Dynamics and oscillations from the load Q and hoisting mechanism are passed on girders. In Fig.16 to Fig.18 are shown graphical results for Front Girder. Results of Rear Girder (Fig.4) are similar with ones of Front girder. Conclusions based on graphs Fig.16, 17 are similar to ones for Crane's base and wheels. Another important conclusion is that oscillations occurring on Load *Q* and cables are passed in other parts of crane with similar form of curve, periods, and frequencies.

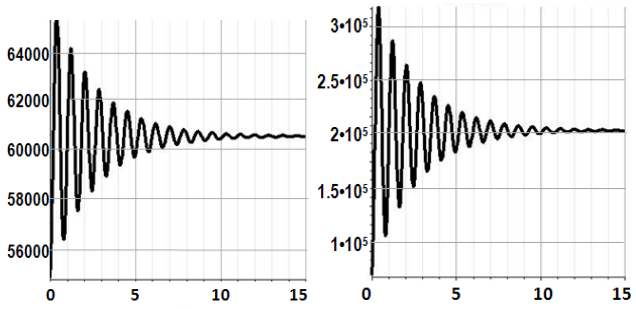

Fig.16. Torque T(x) and T(z) in Crane's Front Girder

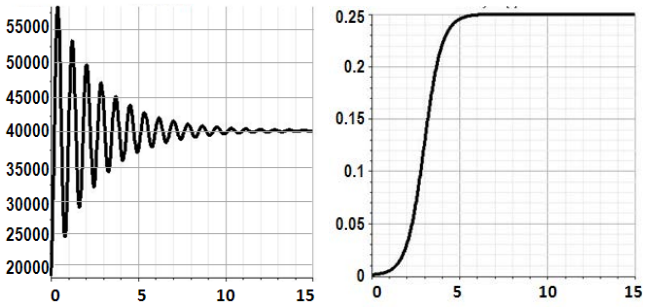

Fig.17. Vertical force component F(y) *Fig.18. Girder Velocity v(z)*

6. Conclusions

The main problem in gantry cranes during travel are oscillations as dynamic occurrences. It is important to identify and regulate them. To do this we created crane model with schematic design and 3-D visualization. Important part of analysis is finding proper simulations plan that reflects real crane's travel motion, so that results are reliable. Results are gained for main dynamic parameters and compared with experimental measurements. From results can be concluded that oscillations in all parts of crane are heavy and mostly with irregular occurrence. They occur in different planes. Oscillations have high intensity at the start of travel process, and small values at end of process [7]. Minimizing oscillations was achieved through planning of travel velocity, parameters of hoisting mechanism, and numerous simulations, in order to find optimal travel [4], [5]. This is done with the aim to optimize the velocity of crane that is main parameter for regulation and optimization. This work is also important for safety at work with gantry cranes. It can be used also for further optimization analysis, and in the future can be used for other work processes like load lifting and cart travel.

7. References

[1] Gantry crane manual, KR-PAV-YR-HK-12H of manufacturer *Kren vinç*, Turkey.

[2] Renuka V. S.& Abraham T Mathew, *Precise Modeling of a Gantry Crane System Including Friction, 3D Angular Swing and Hoisting Cable Flexibility*, IJTARME, Volume-2, Issue-1, 2013.

[3] *MapleSim User Guide*, Maplesoft, a division of Waterloo Maple Inc., 2014.

[4] Doçi Ilir, Lajqi Naser, *Truck mounted cranes during load lifting – dynamic analysis and regulation using modeling and simulations*, MTM Journal 2016, Issue 8 / 2016, p.12.

[5] S. Joe Qin, Badgwell Th.A., *An overview of industrial model predictive control technology*, Control Engineering Practice, A Journal of IFAC, ISSN: 0967-0661, 2003.

[6] Garcíaorden, J. Carlos, Goicolea, José M., Cuadrado Javier, *Multibody Dynamics, Computational methods and app*lications, p.91, 2007 Springer.

[7] Ilir Doci, Beqir Hamidi, Jeton Zeka, *Influence of load swinging on dynamic behavior of l-type portal cranes during forward travelling*, MTM Journal, Issue 7/2015, p.69.

[8] http://www.diniargeo.com/men/scales/weight-indicators.aspx